Robustness Analysis of Nonlinear Systems Along Uncertain Trajectories ⋆

F. Biertümpfel * **J. Theis** ** **H. Pfifer** *

* *Chair of Flight Mechanics and Control, Technische Universität Dresden, 01069 Dresden, Germany (e-mail:{felix.biertuempfel,harald.pfifer}@tu-dresden.de)*
** *Functional Avionics Engineering & GNC, Airbus Defence and Space, 28199 Bremen, Germany (e-mail: julian.theis@airbus.com)*

Abstract: The paper presents a novel approach for robustness analysis of nonlinear dynamic systems in the vicinity of a reference trajectory. The approach linearizes the system with respect to a nominal trajectory and calculates a guaranteed upper bound on the worst-case gain. In contrast to existing methods rooted in linear time-varying systems analysis, the approach accurately includes perturbations that drive the system away from the reference trajectory. The approach further includes a bound for the error associated with the time-varying linearization. Hence, the results obtained in the linear framework provide a valid upper bound for the worst-case performance of the nonlinear system. The calculation of the upper bound relies on the dissipation inequalities formulated in the framework of integral quadratic constraints. It is therefore computationally much cheaper than sample-based methods such as Monte Carlo simulation. The feasibility of the approach is demonstrated on a numerical example.

Keywords: Robustness Analysis, Time-Varying Systems, Uncertain Systems

1. INTRODUCTION

Numerous engineering problems require a system to follow a predefined trajectory. Examples include robotic manipulators (Hošovský et al., 2016), aircraft on final approach (Biertümpfel and Pfifer, 2022), missiles (He et al., 2015), space launch vehicles (Biertümpfel et al., 2021), and vehicles for atmospheric re-entry (Juliana et al., 2004). The performance of such systems depends on how accurate the trajectory is tracked. Uncertainties and disturbances can cause the system to diverge from the predefined trajectory. For example, the ascent trajectory of a launch vehicle is calculated specifically for the mass of the vehicle and will be different if the mass is different. Thus, robustness analysis is an important tool to ensure that the system works as intended.

System dynamics are usually modeled by nonlinear differential equations. Robustness analyses for these models require numerical simulation and some kind of sample-based representation of the uncertainties and disturbances. This is the prevalent "Monte Carlo" approach widely applied in industry. It requires a very large number (often several millions) of simulations to obtain statistically sound analysis results, see, e.g, Theis et al. (2018). One approach to reduce the number of simulations and hence decrease the time required to perform analyses is worst-case optimization. Here, disturbances and uncertain parameters are varied as the result of a numerical optimization with the goal to maximize their adverse effect on performance, see, e.g, Menon et al. (2009). However, neither of these approaches is guaranteed to find the actual worst-case. The Monte Carlo approach can simply miss the worst-case due to the inherent incompleteness of sampling and worst-case optmization is prone to converging to local optima. Other approaches make use of the both computationally and theoretically more tractable linear system theory where methods to calculate actual upper bounds for robust performance exist. The first step towards such an analysis is the Jacobian linearization of the nonlinear differential equations with respect to the trajectory. This results in a finite horizon linear time-varying (LTV) system whose state space representation is a known function of time.

Multiple approaches to assess robust performance of LTV systems exist, e.g., analysis via gap metric in Cantoni and Pfifer (2017) and via integral quadratic constraints (IQCs) in Jönsson (2001). Recent approaches are based on an extension of the LTV bounded-real lemma to IQCs by Moore (2015) and Fry et al. (2017). A closely related formulation is used in Section 3. However, the analysis approaches so far are only concerned with the effect of uncertainties in the state space representation. They are not able to completely recover the behavior of the nonlinear system when parameters are varied along the trajectory. In many applications, however, uncertain parameter-variations are the driving factor for divergence from a nominal trajectory. For example, a space launch vehicle can be thought of as having a nominal mass trajectory during ascent where fuel is burned. Due to inevitable uncertainties in the model of the propulsion system, the true mass trajectory will be different from the nominal one and this causes the launch vehicle to diverge from the desired state trajectory.

The present paper extends the LTV robustness analysis framework to include such effects. This is achieved by augmenting the state space of the LTV system with a constant driving term and including the terms associated with the parameter variation as part of the state matrix. By covering these terms with norm-bounded uncertainties, a form amenable to existing analysis

⋆ This work was supported in part by the European Space Agency under OSIP Contract No. 4000135/85/21/NL/GL/my. The ESA technical officer is Samir Bennani.

methods is then obtained. Specifically, the analysis problem is shown in Section 2 to become a worst-case gain calculation under uncertain initial conditions. Furthermore, the effects of the linearization error along the trajectory are included in a similar way. This makes it possible to relate the results of the linear analysis in a meaningful way back to the nonlinear robust performance analysis problem. In other words, an actual bound on the worst-case performance of the nonlinear system is obtained using linear analysis tools.

The approach bears similarities with first-order trajectory sensitivity analysis, see, e.g., Geng and Hiskens (2019). Such approaches model parameter variation along the trajectory as an additional disturbance input. However, these approaches do not consider the combination with external disturbances that are a key feature of robust performance analysis. The novel approach is also related to the work of Schweidel et al. (2021), who introduce a driving term to model divergence from the trajectory. However, their approach is limited to a pre-sampled uncertainty set and requires a linear fractional representation of the model. This means, the analysis is restricted to previously fixed parameter trajectories which causes an incomplete-sampling issue similar to the Monte-Carlo approach. Including bounds for the linearization error in analyses has been previously suggested by Takarics and Seiler (2015).

In summary, the present paper explicitly considers the effects of parameter variation on the state trajectory and also includes the uncertaintiy associated with the linearization error. It extends the LTV robustness analysis framework for providing an upper bound on the worst-case performance of nonlinear systems in the vicinity of a reference trajectory. The approach is demonstrated on a numerical example in Section 4.

2. PROBLEM FORMULATION

Consider a nonlinear system whose dynamics are defined by the nonlinear ordinary differential equations (ODEs)

$$\begin{aligned} \dot{x}(t) &= f(x(t), d(t), \rho(t)) \\ e(t) &= h(x(t), d(t), \rho(t)). \end{aligned} \tag{1}$$

In (1), the signals $x(t) \in \mathbb{R}^{n_x}$, $d(t) \in \mathbb{R}^{n_d}$, and $e(t) \in \mathbb{R}^{n_e}$ describe the state variable, the input, and the output, respectively. The vector $\rho(t) \in \mathbb{R}^{n_\rho}$ denotes a time-varying parameter vector. A common problem in applied control engineering is to analyze the worst-case performance of the system (1) about a known reference trajectory $\mathcal{T} := \{x(t) = x_\mathcal{T}(t) \wedge d(t) = d_\mathcal{T}(t) \wedge \rho(t) = \rho_\mathcal{T}(t)\ \forall\, t \in [0, T]\}$ over the finite time horizon $[0, T]$. The reference trajectory corresponds to a unique solution that satisfies (1):

$$\begin{aligned} \dot{x}_\mathcal{T}(t) &= f(x_\mathcal{T}(t), d_\mathcal{T}(t), \rho_\mathcal{T}(t)) \\ e_\mathcal{T}(t) &= h(x_\mathcal{T}(t), d_\mathcal{T}(t), \rho_\mathcal{T}(t)) \quad \forall t \in [0, T]. \end{aligned} \tag{2}$$

The worst-case analysis is concerned with perturbations d_Δ and ρ_Δ in the input and parameter vectors, respectively:

$$d_\Delta(t) := d(t) - d_\mathcal{T}(t), \quad \rho_\Delta(t) := \rho(t) - \rho_\mathcal{T}(t). \tag{3}$$

The parameter perturbation ρ_Δ is confined to a set $\mathcal{P} \subset \mathbb{R}$.

The worst-case performance, with respect to the output e at final time T, of the nonlinear system over all possible parameter and input perturbations along the trajectory $\mathcal{T}$ can be expressed as

$$\sup_{\rho_\Delta \in \mathcal{P}} \sup_{\substack{d_\Delta \in L_2[0,T] \\ d_\Delta \neq 0 \\ x(0) = x_\mathcal{T}(0)}} \frac{\|e(T)\|_2}{\|d_\Delta(t)\|_{2[0,T]}}. \tag{4}$$

Here, $\|d_\Delta(t)\|_{2[0,T]} = \sqrt{\int_0^T d_\Delta^T(t) d_\Delta(t)\, dt}$ is the finite horizon L_2-norm of the input perturbation and $\|e(T)\|_2 = \sqrt{e^T(T)e(T)}$ is the Euclidean norm of the output at the terminal time. Computing the worst-case gain (4) is, in general, only possible with a form of sample-based method. Common examples include Monte Carlo simulations or nonlinear worst-case optimization.

Alternatively, the worst-case gain can be approximated using analysis methods for finite horizon LTV systems. This requires a Taylor series expansion of f and h along the trajectory $\mathcal{T}$. Define $x_\Delta(t) := x(t) - x_\mathcal{T}(t)$. The expansion is

$$\begin{aligned} \dot{x} =& \dot{x}_\mathcal{T} + \left.\frac{\partial f}{\partial x}\right|_\mathcal{T} x_\Delta + \left.\frac{\partial f}{\partial d}\right|_\mathcal{T} d_\Delta + \left.\frac{\partial f}{\partial \rho}\right|_\mathcal{T} \rho_\Delta + \epsilon_f \\ e =& e_\mathcal{T} + \left.\frac{\partial h}{\partial x}\right|_\mathcal{T} x_\Delta + \left.\frac{\partial h}{\partial d}\right|_\mathcal{T} d_\Delta + \left.\frac{\partial h}{\partial \rho}\right|_\mathcal{T} \rho_\Delta + \epsilon_h. \end{aligned} \tag{5}$$

Here, ϵ_f and ϵ_h denote the Taylor expansion's higher-order terms and $\left.\frac{\partial f}{\partial x}\right|_\mathcal{T}$ denotes the Jacobian of f with respect to x evaluated along the reference trajectory $\mathcal{T}$. The other Jacobians are defined accordingly. The common LTV state space representation

$$\begin{aligned} \dot{x}_\Delta(t) &= A(t)\, x_\Delta(t) + B(t)\, d_\Delta(t) \\ e_\Delta(t) &= C(t)\, x_\Delta(t) + D(t)\, d_\Delta(t) \end{aligned} \tag{6}$$

is obtained by neglecting the higher-order terms ϵ_f and ϵ_h, and assuming nominal parameters, i.e., $\rho_\Delta(t) = 0$ for $t \in [0, T]$. In (6), the perturbed output is $e_\Delta = e - e_\mathcal{T}$ and the system matrices are

$$\begin{aligned} A(t) &= \left.\frac{\partial f}{\partial x}\right|_\mathcal{T}, \; B(t) = \left.\frac{\partial f}{\partial d}\right|_\mathcal{T}, \\ C(t) &= \left.\frac{\partial h}{\partial x}\right|_\mathcal{T}, \; D(t) = \left.\frac{\partial h}{\partial d}\right|_\mathcal{T}. \end{aligned} \tag{7}$$

The gain of the LTV system (6) defined as

$$\sup_{\substack{d_\Delta \in L_2[0,T] \\ d_\Delta(t) \neq 0, x_\Delta(0) = 0}} \frac{\|e_\Delta(T)\|_2}{\|d_\Delta(t)\|_{2[0,T]}} \tag{8}$$

can be readily computed as for instance described in Green and Limebeer (1995). The gain (8) relates perturbations in the input to deviations from the nominal output $e_\mathcal{T}$. Since the reference output is known and $\|e(T)\|_2 \leq \|e_\mathcal{T}(T)\|_2 + \|e_\Delta(T)\|_2$, the result can, in principle, be used to establish an upper bound on the robust performance metric (4). However, as this analysis does not consider parameter perturbations and further neglects the higher-order terms of the Taylor series expansion, no actual guarantees are provided.

Remark 1. Uncertainties in the state space system (6) are frequently included in an attempt to account for the neglected parameter variation and higher-order terms. Examples are dynamic input uncertainties (Seiler et al., 2019) or parametric uncertainties (Biertümpfel et al., 2021). This approach leads to a worst-case LTV analysis over the newly introduced uncertainty set. However, such uncertainties alone cannot drive the system state away from the trajectory: $e_\Delta(t) = \dot{x}_\Delta(t) = 0$ as long as $d_\Delta(t) = 0$. In contrast, a parameter variation ρ_Δ in (1) leads to a variation in $\dot{x}(t)$. This effect cannot be accurately represented by such uncertainties.

Unlike the common approach described so far, the method in this paper explicitly considers perturbations from the reference trajectory, i.e., $\rho_\Delta(t) \neq 0$ and bound the higher-order terms ϵ_f

and ϵ_h. Hence, it can be used to calculate guaranteed bounds on the worst-case performance metric of the nonlinear system (4).

3. LTV WORST-CASE ANALYSIS FOR PERTURBED TRAJECTORIES

In order to account for the parameter perturbation ρ_Δ in the linear analysis, the state space representation (6) can be extended as follows. First, define

$$E(t) = \left.\frac{\partial f}{\partial \rho}\right|_{\mathcal{T}}, \; F(t) = \left.\frac{\partial h}{\partial \rho}\right|_{\mathcal{T}}. \tag{9}$$

With this, the Taylor series expansion (5) can be written as

$$\begin{aligned} \dot{x} =& \dot{x}_{\mathcal{T}} + A\, x_\Delta + B\, d_\Delta + E\, \rho_\Delta + \epsilon_f \\ e =& e_{\mathcal{T}} + C\, x_\Delta + D\, d_\Delta + F\, \rho_\Delta + \epsilon_h. \end{aligned} \tag{10}$$

A state space model for (10) is obtained by augmenting the state vector x_Δ with a constant driving term:

$$\begin{aligned} \begin{bmatrix} \dot{x}_\Delta \\ 0 \end{bmatrix} &= \begin{bmatrix} A & E\rho_\Delta + \epsilon_f \\ 0 & 0 \end{bmatrix} \begin{bmatrix} x_\Delta \\ 1 \end{bmatrix} + \begin{bmatrix} B \\ 0 \end{bmatrix} d_\Delta \\ e_\Delta &= \begin{bmatrix} C & F\rho_\Delta + \epsilon_h \end{bmatrix} \begin{bmatrix} x_\Delta \\ 1 \end{bmatrix} + D\, d_\Delta. \end{aligned} \tag{11}$$

This model is a completely equivalent representation for (10). It is non-standard due to the constant driving term appearing in the state vector. This trick, however, allows the parameter variation to excite the system dynamics independently of the disturbances. In a next step, the driving term is replaced by a state variable x_ρ confined to $\mathcal{U} := \{x_\rho \in \mathbb{R} \,|\, x_\rho^2 \leq 1\}$:

$$\begin{aligned} \begin{bmatrix} \dot{x}_\Delta \\ 0 \end{bmatrix} &= \begin{bmatrix} A & E\rho_\Delta + \epsilon_f \\ 0 & 0 \end{bmatrix} \begin{bmatrix} x_\Delta \\ x_\rho \end{bmatrix} + \begin{bmatrix} B \\ 0 \end{bmatrix} d_\Delta \\ e_\Delta &= \begin{bmatrix} C & F\rho_\Delta + \epsilon_h \end{bmatrix} \begin{bmatrix} x_\Delta \\ x_\rho \end{bmatrix} + D\, d_\Delta. \end{aligned} \tag{12}$$

The introduction of x_ρ leads to a homotopy-like analysis that covers all parameter perturbations and higher-order errors from the nominal LTV performance to the maximum bounds. In other words, the influence of the parameter variation and the higher-order terms vanishes for $x_\rho = 0$ and is completely recovered for $x_\rho = 1$.

It has already been established that the parameter perturbations ρ_Δ are constrained to some bounded set $\mathcal{P}$. Note that the higher-order terms of the Taylor series expansion, ϵ_f and ϵ_h, are small for reasonably small variations from the reference trajectory. Assume that a bound at each point in time can be found and thus that they are confined to sets $\mathcal{E}_f$ and $\mathcal{E}_h$, respectively. Takarics and Seiler (2015) propose a formal bound on ϵ_f and ϵ_h based on the Lipschitz constant of the nonlinear system. Alternatively, sampling can be used to obtain such a bound. In either case, the terms ρ_Δ, ϵ_f, and ϵ_h can now be treated as time-varying norm-bounded uncertainties. The worst-case gain of (12) can be calculated as

$$\sup_{\substack{\rho_\Delta \in \mathcal{P} \\ \epsilon_f \in \mathcal{E}_f \\ \epsilon_h \in \mathcal{E}_h}} \; \sup_{\substack{d_\Delta \in L_2[0,T] \\ d_\Delta(t) \neq 0 \\ x_\Delta(0)=0, x_\rho \in \mathcal{U}}} \frac{\|e_\Delta(T)\|_2}{\|d_\Delta(t)\|_{2[0,T]}} \tag{13}$$

Together with the nominal output, this now provides an actual upper bound for the robust performance of the nonlinear system (1). Note that the state x_ρ requires a non-zero initial condition to take effect. Since all "actual" state variables have zero initial conditions for the worst-case gain (13), the uncertain LTV system (12) has only partially uncertain initial conditions.

The uncertain state space model (12) can be transformed into a linear fractional representation (LFR), pictured in Fig. 1. This LFR is written as $F_u(G, \Delta)$ and can be interpreted as the feedback interconnection of the nominal dynamics of (11), denoted by G, and the uncertainties, denoted by Δ. The uncertainty Δ is

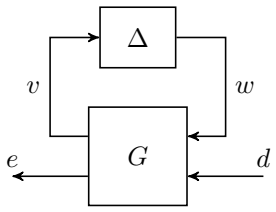

Fig. 1. Linear fractional representation of uncertain LTV system

block-diagnonal and its elements Δ_i represent the components of ρ_Δ, ϵ_f, and ϵ_h, where the entries corresponding to ρ_Δ can be repeated. As is common practice in robustness analysis, the precise relation between the inputs v and outputs w of the uncertainty Δ is replaced by constraints on the input/output behavior. Ultimately, this replacement leads to computationally tractable conditions to compute upper bounds on the worst-case gain (13) later on.

For now, assume that v_i and w_i are the input and output of the i^{th} uncertainty entry $\Delta_i = \delta_i I_{n_i}$, respectively, i.e. $w_i = \Delta_i v_i$. Further let the uncertainty be bounded by $|\delta_i(t)| \leq b_i(t) \in \mathbb{R}^+$ and arbitrarily fast time-varying. A constraint on v_i and w_i that guarantees the boundedness of δ_i is given pointwise in time as

$$\begin{bmatrix} v_i \\ w_i \end{bmatrix}^T \begin{bmatrix} b_i^2 X_i & Y_i \\ Y_i^T & -X_i \end{bmatrix} \begin{bmatrix} v_i \\ w_i \end{bmatrix} \geq 0 \quad \forall t \in [0, T], \tag{14}$$

where $X_i = X_i^T > 0$ and $Y_i = -Y_i^T$ are so-called multipliers of appropriate dimension. These multipliers can be time-varying. It is straightforward to show that (14) guarantees $|\delta_i(t)| \leq b_i(t)$ for any choice of X_i and Y_i, see for instance Veenman et al. (2016). The values of the multipliers have a direct impact on the bound calculation at the end of the section. Thus, they will be used as free parameters in a semidefinite optimization problem to find the smallest upper bound on the worst-case gain.

The quadratic constraint (14) for a single entry Δ_i is extended to the whole uncertainty block Δ in the following way assuming k entries in Δ. A new vector signal z is defined by stacking all pairs v_i, w_i, i.e. $z^T = \begin{bmatrix} \begin{bmatrix} v_1^T & w_1^T \end{bmatrix}, \ldots, \begin{bmatrix} v_k^T & w_k^T \end{bmatrix} \end{bmatrix}^T$. Additionally, a multiplier matrix M stacks all the individual multipliers on its block diagonal such that

$$M = \begin{bmatrix} \begin{bmatrix} b_1^2 X_1 & Y_1 \\ Y_1^T & -X_1 \end{bmatrix} & & \\ & \ddots & \\ & & \begin{bmatrix} b_k^2 X_k & Y_k \\ Y_k^T & -X_k \end{bmatrix} \end{bmatrix}. \tag{15}$$

Using these definitions for z and M, the input/output behavior of Δ can then be bounded by the pointwise-in-time quadratic constraint $z^T M z \geq 0$ for all $t \in [0, T]$. Thus, the uncertainty in the interconnection $F_u(G, \Delta)$ of Fig. 1 can be replaced by adding w and z as additional external input and output, respectively, where the output z must satisfy the quadratic

constraint defined by M. The so-extended state space model is written as:

$$\begin{aligned}\begin{bmatrix}\dot{x}_\Delta\\0\end{bmatrix} &= \hat{A}\begin{bmatrix}x_\Delta\\x_\rho\end{bmatrix} + \begin{bmatrix}\hat{B}_1 & \hat{B}_2\end{bmatrix}\begin{bmatrix}w\\d_\Delta\end{bmatrix}\\ \begin{bmatrix}z\\e_\Delta\end{bmatrix} &= \begin{bmatrix}\hat{C}_1\\\hat{C}_2\end{bmatrix}\begin{bmatrix}x_\Delta\\x_\rho\end{bmatrix} + \begin{bmatrix}\hat{D}_{11} & \hat{D}_{12}\\\hat{D}_{21} & \hat{D}_{22}\end{bmatrix}\begin{bmatrix}w\\d_\Delta\end{bmatrix}\end{aligned} \tag{16}$$

with

$$z^T M z \geq 0 \quad \forall t \in [0,T]. \tag{17}$$

Remark 2. The quadratic constraints given in this section generalize into the well-known IQC framework. Specifically, the constraint (17) holds for each point in time. Thus, integrating it over the time interval must also satisfy the constraint, i.e. $\int_0^T z^T M z dt \geq 0$. Using this more general integral quadratic form would allow the combination of different types of uncertainties in the analysis, e.g. time delays or uncertainties in the original nonlinear system. For the sake of readability, the use of the IQC form is not further pursued in this paper.

The following Theorem 1, based on the extended system (16), provides an analysis condition to calculate an upper bound on the worst-case gain (13).

Theorem 1. Let $F_u(G,\Delta)$ be well posed $\forall\,\Delta$ satisfying the quadratic constraint (17). Then the worst-case gain (13) is bounded by the scalar $\gamma > 0$ if there exist a continuously differentiable symmetric matrix function $P = \begin{bmatrix}P_{11} & P_{12}\\P_{12}^T & P_{22}\end{bmatrix}: \mathbb{R}_0^+ \to \mathbb{R}^{(n_x+1)\times(n_x+1)}$ as well as scalar constants $\alpha_1 > 0$ and $\alpha_2 > 0$ such that

$$\begin{bmatrix}\dot{P}+P\hat{A}+\hat{A}^TP & P\hat{B}_1 & P\hat{B}_2\\ \hat{B}_1^TP & 0 & 0\\ \hat{B}_2^TP & 0 & -I_{n_d}\end{bmatrix} + \begin{bmatrix}\hat{C}_1^T\\\hat{D}_{11}^T\\\hat{D}_{12}^T\end{bmatrix} M \begin{bmatrix}\hat{C}_1^T\\\hat{D}_{11}^T\\\hat{D}_{12}^T\end{bmatrix}^T < 0 \tag{18}$$

and

$$\begin{bmatrix}P_{22}(0)-\alpha_1 & 0 & 0\\ 0 & \alpha_2\hat{C}_2^T(T)\hat{C}_2(T)-P(T) & 0\\ 0 & 0 & \alpha_1-\alpha_2\gamma^2+1\end{bmatrix} < 0. \tag{19}$$

Proof. Theorem 1 is a corollary of Theorem 2.3 in Moore (2015). The proof provided there requires only minor modifications.

The theorem of Moore (2015) is concerned with uncertain initial conditions for all states. For the application to the worst-case gain calculation, the initial conditions for x are zero and only the single initial condition for the pseudo-state x_ρ that represents the driving term needs to be considered. This is done in Theorem 1 through the partitioning of P into an $n_x \times n_x$ matrix P_{11} (related to x) and a scalar P_{22} (related to x_ρ). The upper left entry in (19) thus corresponds to the constraint on $x_\rho(0)$.

The condition (18) has to hold for all $t \in [0,T]$ and therefore presents an infinite number of LMI constraints. The state-of-the-art approach to circumvent this problem enforces the condition only on a finite number of grid points $t_i \in [0,T]$, see, e.g., Pfifer and Seiler (2016). The decision variables in conditions (18) and (19) are the matrix function P, the multiplier matrices X_i and Y_i from (15), as well as α_1 and α_2. The time-dependent functions P, X_i, and Y_i must also be constrained to a finite dimensional subspace to allow a computational solution. Most commonly, these are expressed as linear combinations, e.g. $P(t) = \sum_{i=0}^{N_b} t^i P_i$, $i = 0,1,...,N_b$. Thus, the coefficient matrices become the decision variables. Alternatively, more sophisticated basis functions such as cubic splines can be used, see Seiler et al. (2019). Feasible coefficients can be calculated as a semidefinite program with the constraints (18) and (19) for a given γ. A bisection over γ identifies the minimal feasible upper bound.

4. NUMERICAL EXAMPLE

The example concerns the robustness analysis of a pendulum along a prescribed trajectory. The penduluum has a constant length $l = 1.25\,\mathrm{m}$ and is acted upon by gravity ($g = 9.81\,\frac{\mathrm{m}}{\mathrm{s}^2}$) and by a tangential force F. The aim of the analysis is to calculate the worst-case deflection angle ϕ at the final time T due to a disturbance in the force F. The pendulum's mass m (kg) and damping σ (kg $\cdot$ m^2/s) vary with time. They constitute the exogenous parameter vector ρ for this example. The motion of the pendulum is described by the following nonlinear differential equations:

$$\begin{aligned}\begin{bmatrix}\dot{\phi}\\\ddot{\phi}\end{bmatrix} &= \begin{bmatrix}\dot{\phi}\\\frac{F\cos\phi}{ml} - \frac{g\sin\phi}{l} - \frac{\sigma\dot{\phi}}{ml^2}\end{bmatrix}\\ e &= \phi.\end{aligned} \tag{20}$$

A reference trajectory over 10 s is obtained in the following way: The reference deflection angle and rate are initialized as $\phi_\mathcal{T}(0) = 45°$ and $\dot{\phi}_\mathcal{T}(0) = 0°/\mathrm{s}$, respectively. For the exogenous parameters, the following trajectory is defined:

$$\rho_\mathcal{T} = \begin{bmatrix}m_\mathcal{T}\\\sigma_\mathcal{T}\end{bmatrix} = \begin{bmatrix}3-0.1t\\2+0.25t\end{bmatrix}. \tag{21}$$

Lastly, the force is set to the constant value $F_\mathcal{T} = 29.43\,\mathrm{N}$. Using these specifications, the nonlinear differential equations (20) are integrated along the reference trajectory to obtain $\phi_\mathcal{T}$ and $\dot{\phi}_\mathcal{T}$. Note that even with a constant force acting on the pendulum, the variations in the mass and damping still cause a motion. While it is assumed that the damping is accurately known, the mass variation m_Δ about the reference trajectory is considered $\pm 0.25\,\mathrm{kg}$ uncertain in this example.

Linearizing the nonlinear system (20) along $\mathcal{T}$ yields the LTV system

$$\begin{aligned}\begin{bmatrix}\dot{\phi}_\Delta\\\ddot{\phi}_\Delta\\0\end{bmatrix} &= \begin{bmatrix}0 & 1 & 0\\ -\frac{g}{l\cos\phi_\mathcal{T}} & -\frac{\sigma_\mathcal{T}}{m_\mathcal{T}l^2} & (\frac{\sigma_\mathcal{T}}{m_\mathcal{T}^2l^2} - \frac{\cos\phi_\mathcal{T}F_\mathcal{T}}{m_\mathcal{T}^2l})m_\Delta + \epsilon_{\ddot{\phi}}\\ 0 & 0 & 0\end{bmatrix}\begin{bmatrix}\phi_\Delta\\\dot{\phi}_\Delta\\x_\rho\end{bmatrix}\\ &\quad + \begin{bmatrix}0\\\frac{\cos\phi_\mathcal{T}}{m_\mathcal{T}l}\\0\end{bmatrix}F_\Delta\\ e_\Delta &= \begin{bmatrix}1 & 0 & 0\end{bmatrix}\begin{bmatrix}\phi_\Delta\\\dot{\phi}_\Delta\\x_\rho\end{bmatrix}.\end{aligned} \tag{22}$$

The higher-order terms of the Taylor series are represented by $\epsilon_{\ddot{\phi}}$. A reasonable bound for $\epsilon_{\ddot{\phi}}$ is identified by sampling the nonlinear dynamics (20) around the reference trajectory and calculating the maximum linearization errors. For this

example, the linearization error is calculated for dispersions $\pm 10°$, $\pm 5°/\mathrm{s}$, $\pm 0.25\,\mathrm{kg}$, and $\pm 0.5\,\mathrm{N}$ around $\phi_{\mathcal{T}}(t)$, $\dot{\phi}_{\mathcal{T}}(t)$, $m_{\mathcal{T}}(t)$, and $F_{\mathcal{T}}(t)$, respectively. A time-dependent bound $b_\epsilon(t)$ is obtained from the pointwise-in-time linearization errors. This leads to $|\epsilon_{\ddot{\phi}}(t)| \leq b_\epsilon(t)$. The bound starts at $0.25\,\mathrm{rad/s^2}$ for $t = 0\,\mathrm{s}$ and ends at $0.63\,\mathrm{rad/s^2}$ at $t = 10\,\mathrm{s}$.

First, a Monte Carlo simulation of the nonlinear model is performed to establish a baseline for comparison. The nonlinear model is simulated with 3465 unique combinations of norm-bounded disturbances ($\|F_\Delta\|_{2[0,T]} = 1$) and time-varying mass in the range of $\pm 0.25\,\mathrm{kg}$ around $m_{\mathcal{T}}(t)$. Fig. 2 shows selected time series of the calculated deviations ϕ_Δ (——) from the reference trajectory $\phi_{\mathcal{T}}$. The Monte Carlo simulation yields a maximum deviation of $16.2°$. It requires a computational time of 249 s on a standard desktop PC.

Next, the proposed worst-case calculation from Section 3 is applied. The extended state space system (16) with the quadratic constraint (17) is analyzed with Theorem 1. A third-order polynomial basis function is used to represent P, X_i, and Y_i. The conditions of Theorem 1 are evaluated on a grid with a density of 0.1 s. The resulting semidefinite program is solved using Matlab's `lmilab`. A bisection over γ yields $\gamma = 31.2°$. The complete bisection takes 18 s on the same computer. This value is the upper bound on the terminal deviation $\phi_\Delta(T)$ for all disturbances with $\|F_\Delta\|_{2[0,T]} = 1$. Fig. 2 shows that all simulation results remain inside this bound.

Finally, a "conventional" LTV analysis is performed for comparison. For this analysis, the pendulum is linearized without accounting for the parameter variation and the higher-order terms, leading to the standard LTV model (6). The state space matrices in this models are functions of the reference mass $m_{\mathcal{T}}$. A standard approach is to consider this dependence as uncertain. In other words, an uncertain mass variation of $\pm 0.25\,\mathrm{kg}$ is added to all entries $m_{\mathcal{T}}$ in the state space matrices. Note that this is not the same as directly including the mass perturbation m_Δ in the linearization. The worst-case gain (8) of this uncertain LTV system is calculated by sampling the mass and applying the results of Green and Limebeer (1995). The analysis yields $\gamma = 2.4°$ which is clearly violated by the actual simulation results, see again Fig. 2.

Note that the proposed worst-case analysis appears to be more conservative than the Monte Carlo simulation. This is due to two main reasons. First, the Monte Carlo simulation can only provide a *lower* bound for the worst-case performance, not an upper bound. In other words, the performance cannot be better than the worst-case obtained in Monte Carlo simulation, but it could be worse. As previously discussed, this analysis depends heavily on the sampling of the disturbances and perturbations. In contrast, the proposed analysis provides a guaranteed *upper* bound on the worst-case performance. This bound is also obtained in a fraction of time (14-times faster) compared to the Monte-Carlo simulation. Second, the proposed analysis considers arbitrarily fast time-varying perturbations, whereas the samples in the Monte Carlo simulation have finite variation rates. Conservatism could thus be reduced by considering rate-bounded parametric uncertainties, see, e.g., Veenman et al. (2016).

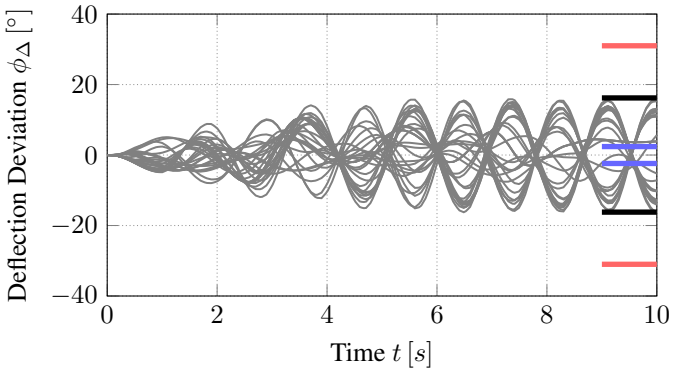

Fig. 2. Representative Monte Carlo simulation samples (——), most critical Monte Carlo result (——), upper bound from proposed method (——), conventional analysis (——)

5. CONCLUSION

The paper presents a novel approach for the analysis of nonlinear systems along uncertain trajectories. It formulates time-varying parameter deviations from the nominal trajectory as uncertain initial conditions of an extended state space system in conjunction with time-varying uncertainties. The time-varying uncertainties can be bounded by quadratic constraints, which belong to the general IQC framework. Hence, the resulting uncertain LTV system can be efficiently analyzed in the LTV IQC framework. A numerical example demonstrates that the approach requires significantly less computational effort than a Monte Carlo analysis and indeed provides an upper bound for the worst-case performance.

REFERENCES

Biertümpfel, F., Bennani, S., and Pfifer, H. (2021). Time-varying robustness analysis of launch vehicles under thrust perturbations. *Advanced Control for Applications*, 3(4). doi: 10.1002/adc2.93.

Biertümpfel, F. and Pfifer, H. (2022). Finite horizon analysis of autolanded aircraft in final approach under crosswind. *Control Engineering Practice*, 122. doi: 10.1016/j.conengprac.2022.105105.

Cantoni, M. and Pfifer, H. (2017). Gap metric computation for time-varying linear systems on finite horizons. *IFAC-PapersOnLine*, 50(1), 14513 – 14518. doi: https://doi.org/10.1016/j.ifacol.2017.08.2073.

Fry, J.M., Farhood, M., and Seiler, P. (2017). IQC-based robustness analysis of discrete-time linear time-varying systems. *International Journal of Robust and Nonlinear Control*, 27(16), 3135–3157. doi:10.1002/rnc.3731.

Geng, S. and Hiskens, I.A. (2019). Second-order trajectory sensitivity analysis of hybrid systems. *IEEE Transactions on Circuits and Systems I: Regular Papers*, 66(5), 1922–1934. doi:10.1109/tcsi.2019.2903196.

Green, M. and Limebeer, D.J.N. (1995). *Linear Robust Control*. Prentice-Hall, Inc., Upper Saddle River, NJ, USA.

He, F., Wang, L., Yao, Y., Qi, H., and Jiang, Z. (2015). Analysis and design of linear time-varying systems based on a finite-time performance index. In *2015 American Control Conference (ACC)*, 5948–5953. doi:10.1109/ACC.2015.7172273.

Hošovský, A., Piteľ, J., Židek, K., Tóthová, M., Sárosi, J., and Cveticanin, L. (2016). Dynamic characterization and simulation of two-link soft robot arm with pneumatic muscles. *Mechanism and Machine Theory*, 103, 98–116. doi: 10.1016/j.mechmachtheory.2016.04.013.

Jönsson, U.T. (2001). Robustness of trajectories with finite time extent. *IFAC Proceedings Volumes*, 34(6), 1077 – 1082. doi: https://doi.org/10.1016/S1474-6670(17)35326-0.

Juliana, S., Chu, Q., Mulder, J., and van Baten, T. (2004). Flight control of atmospheric re-entry vehicle with nonlinear dynamic inversion. In *AIAA Guidance, Navigation, and Control Conference and Exhibit*. American Institute of Aeronautics and Astronautics. doi:10.2514/6.2004-5330.

Menon, P., Prempain, E., Postlethwaite, I., Bates, D., and Bennani, S. (2009). Nonlinear worst-case analysis of an LPV controller for approach-phase of a re-entry vehicle. In *AIAA Guidance, Navigation, and Control Conference*. American Institute of Aeronautics and Astronautics. doi: 10.2514/6.2009-5638.

Moore, R.M. (2015). *Finite horizon robustness analysis using integral quadratic constraints*. Master's thesis, University of California, Berkeley, CA.

Ossmann, D. and Pfifer, H. (2019). Robustness analysis of continuous periodic systems using integral quadratic constraints. In *2019 IEEE 58th Conference on Decision and Control (CDC)*. IEEE.

Pfifer, H. and Seiler, P. (2016). Less conservative robustness analysis of linear parameter varying systems using integral quadratic constraints. *International Journal of Robust and Nonlinear Control*, 26(16), 3580–3594. doi: 10.1002/rnc.3521.

Schweidel, K.S., Buch, J.R., Seiler, P.J., and Arcak, M. (2021). Computing worst-case disturbances for finite-horizon linear time-varying approximations of uncertain systems. *IEEE Control Systems Letters*, 5(5), 1753–1758. doi: 10.1109/lcsys.2020.3043843.

Seiler, P., Moore, R.M., Meissen, C., Arcak, M., and Packard, A. (2019). Finite horizon robustness analysis of LTV systems using integral quadratic constraints. *Automatica*, 100, 135–143. doi:10.1016/j.automatica.2018.11.009.

Takarics, B. and Seiler, P. (2015). Gain scheduling for nonlinear systems via integral quadratic constraints. In *2015 American Control Conference (ACC)*. IEEE. doi: 10.1109/acc.2015.7170834.

Theis, J., Ossmann, D., Thielecke, F., and Pfifer, H. (2018). Robust autopilot design for landing a large civil aircraft in crosswind. *Control Engineering Practice*, 76, 54–64. doi: 10.1016/j.conengprac.2018.04.010.

Veenman, J., Scherer, C.W., and Köroğlu, H. (2016). Robust stability and performance analysis based on integral quadratic constraints. *European Journal of Control*, 31, 1–32. doi:10.1016/j.ejcon.2016.04.004.